Batool Reyhaniyan Zavareh, Alireza Salehirad* and Saeed Mirdamadi

Effects of using the liquid phase method on the physicochemical, mechanical, and bioactivity properties of hydroxyapatite/calcium aluminate bioceramic nanocomposites

DOI 10.1515/gps-2016-0188
Received October 30, 2016; accepted March 1, 2017; previously published online May 19, 2017

Abstract: In this research, 80 wt.% hydroxyapatite (HA)/20 wt.% calcium aluminate (CA) bioceramic nanocomposites were synthesized by using three liquid phase green methods. X-ray diffraction, energy dispersive X-ray spectroscopy, and field emission-scanning electron microscopy were conducted for the characterization of nanocomposites. To study the mechanical (compressive strength, flexural strength, and hardness) and physical (density, porosity, and water adsorption) properties of nanocomposites, these materials were sintered by spark plasma technique, after which the desired properties were measured. To study the bioactivity of samples, SBF vitro test was used. After reviewing the obtained data, results showed that the bioactivity and mechanical properties of the synthesized HA/NA nanocomposites were improved compared with those of the nanocomponents that form them and those of similar micro-scale composites. The measured maximum compressive strength, flexural strength, and hardness of the synthesized nanocomposites were 440 MPa, 137 MPa, and 202 H_V, respectively. The corresponding amounts for hydroxyapatite nanoparticles were 350 MPa, 115 MPa, and 124 H_V, respectively.

Keywords: bioceramic; calcium aluminate; hydroxyapatite; nanocomposite; synthesis method.

1 Introduction

Hydroxyapatite, $Ca_{10}(PO_4)_6(OH)_2$, is a natural mineral found in the inorganic components of bone and tooth enamel. The main characteristic of hydroxyapatite (HA) is its bioactivity, which gives it the ability to chemically and directly bond with the body's cells. Despite the high bioactivity properties of HA, it does not have good mechanical properties and it is sensitive to the growth of crack in wet environments [1]. One method to improve the mechanical properties of HA is by compositing it with other bioceramics in the nanoscale. Often, HA bioceramics are composited with neutral bioceramics with high mechanical properties. Such ceramics as alumina [2–5], Zirconia [6–9], and Titania [10–12] are neutral biocomposites that are typically composited with hydroxyapatite. Calcium aluminate (CA) is another bioceramic with many biological and medical applications. CA is assessed as a biomaterial because of its physical, mechanical, and overall biocompatibility properties. Owing to their unique hardening/curing characteristic and relevant microstructure, calcium aluminate-based materials have shown great potential as possible biomaterials [13]. CA bioceramics belong to the chemically bonded ceramics known as inorganic cements [13].

Beherei et al. [14] were the first to synthesize HA/CA composites in the micro-scale through the solid-state method. They obtained an 80 wt.% HA/20 wt.% CA composite with improved mechanical properties and bioactivity compared with other components. Recently, Oliveira et al. [15] reported the structural and mechanical properties of HA synthesized through two methods (mechanical and chemical deposition), and compared these properties with those of commercial HA. Furthermore, they added synthetic and commercial HA separately with weight percentages of 1, 2, 4, 6, and 10 wt.% to the CA cement, after which they investigated the mechanical and biological properties of the composites. They reported that these synthesis routes were effective in the preparation of HA and that adding it to CA cement increased sample interaction with the SBF solution, thus reducing overall porosity and pore size due to the deposition of apatite into the sample. In addition to the biological properties, the mechanical properties of CA cement also increased. In the mentioned article, samples were in the micro-scale and the HA and CA were mixed mechanically [15].

***Corresponding author: Alireza Salehirad,** Department of Chemical Technologies, Iranian Research Organization for Science and Technology (IROST), Tehran, Iran, e-mail: salehirad@irost.ir
Batool Reyhaniyan Zavareh: Department of Chemical Technologies, Iranian Research Organization for Science and Technology (IROST), Tehran, Iran
Saeed Mirdamadi: Department of Biotechnology, Iranian Research Organization for Science and Technology (IROST), Tehran, Iran

The main aim of the current study was to improve the mechanical (compressive strength, flexural strength, and hardness) and physicochemical properties of hydroxyapatite. This objective was achieved by using CA nanoparticles or its precursor, which resulted in the creation of HA/CA nanocomposites using three different liquid phase methods as follows:

1. mixing the HA nanoparticles with the CA nanoparticles in the liquid phase (method 1);
2. mixing the HA precursor with the CA nanoparticles (method 2); and
3. mixing the CA precursor with the HA nanoparticles (method 3).

In addition to improving the mechanical and physicochemical properties of HA, its bioactive properties were also improved because the CA used as a bioceramic at the nano-scale had better biocompatibility.

Using the liquid phase method in synthesizing nanocomposites has many advantages, including low cost, low energy consumption, simplicity, easy control of reaction conditions, and environmental compatibility.

2 Materials and methods

2.1 Materials

All chemicals used, including calcium nitrate tetrahydrate, aluminum nitrate nonahydrate, phosphoric acid (85%), ammonium hydroxide (25%), citric acid monohydrate, and ethylene glycol GR, were purchased from Merck (Stuttgart, Germany). The HA:CA weight ratio was 4:1 in all synthesized nanocomposites.

2.2 Synthesis of hydroxyapatite and calcium aluminate nanoparticles

2.2.1 Synthesis of hydroxyapatite nanoparticles: HA was prepared according to the method described by Kong et al. [16]. To an aqueous solution of 0.5 M $Ca(NO_3)_2.4H_2O$, H_3PO_4 with a Ca/P molar ratio of 1.67 was added and the obtained solution was stirred for 30 min. Then, ammonia solution was used to initiate precipitation. The resulting precipitate was washed with distilled water and dried at 70°C for 24 h to obtain the nanoparticles.

2.2.2 Synthesis of calcium aluminate nanoparticles: CA was synthesized based on the procedure reported by Gaki et al. [17]. An aqueous solution was prepared containing $Ca(NO_3)_2.4H_2O$ and $Al(NO_3)_3.9H_2O$ with Ca:Al molar ratio of 1:2 in 100 ml distilled water. Citric acid (Cit) was added to the solution (molar ratio of Cit:total cations was one). Ethylene glycol (EG) in an EG:Cit molar ratio of 2:1 was added to the obtained solution. The resulting solution was continuously stirred at 80°C until a viscous gel was obtained. The obtained gel was dried at 150°C for 24 h and calcined at 900°C for 3 h.

2.3 Synthesis of nanocomposites

2.3.1 Method 1: mixing hydroxyapatite nanoparticles with calcium aluminate nanoparticles in the liquid phase: The desired nanocomposite was synthesized by mixing HA and CA nanoparticles in the liquid phase. Specifically, HA (80 wt.%) and CA nanoparticles (20 wt.%) were mixed in distilled water. The mixture was continuously stirred for 24 h and dried in an oven at 100°C.

2.3.2 Method 2: mixing the hydroxyapatite precursor with the calcium aluminate nanoparticles: To prepare the HA precursor, all the steps in preparing the HA nanoparticles (stated in Section 2.2.1) were performed, except drying. The defined amount of CA nanopowder in the distilled water, which was steadily stirred for 2 h, was added to the wet HA precursor. Here, the amount of the raw materials must be quantified so that the weight ratio of HA to the added CA in the mixture should be 4:1. The resulting mixture was stirred for 4 h and then placed in oven at 70°C for 24 h. The main points of this method were the nanoparticle mixture stirring speed and time, because at a longer time and a higher stirring speed, the HA precursor would be converted to the other phase of calcium phosphate called brushite.

2.3.3 Method 3: mixing the calcium aluminate precursor with the hydroxyapatite nanoparticles: For the preparation of the CA precursor, all the steps of synthesizing the CA nanoparticles, presented in Section 2.2.2, except calcination, were performed. The appropriate amount of HA nanoparticles was added to the obtained precursor in the liquid phase, after which the mixture was stirred for 24 h. After drying, the resulting sample was calcined at 900°C for 3 h.

Other methods were used for these experiments, but all of them failed. One of these methods involved adding the HA nanoparticle to the gel obtained in the CA precursor preparation. Given that the gel structure was destroyed by adding the HA nanoparticle, a black solid was produced after calcination. In another method, the HA nanoparticle was added to the solution a few minutes before the gel formation; however, the HA nanoparticle was dissolved, which may be due to the presence of citric acid in the solution. HA is unstable in citric acid and may be dissolved in this solution depending on the citric acid concentration.

2.4 Characterization

Phase analysis of samples was performed by X-ray diffraction (XRD) technique on an EQUINOX Model 3000 (Inel Company, France) with Kα. λ = 1.541874 Å. The morphologies of the samples were investigated using a field emission scanning electron microscope (FE-SEM, Mira Model, Tskan, Czech Republic). For cooking the samples under 40 MPa and for heating SPS, an SPS 20T-10 Model was used (Serial No. EF120311, Easy Fashion Co.). SPS temperature was measured by using an optical pyrometer, RAYR312MSCL2G. Heat treatment was carried out in a vacuum condition at a heating rate of 50°C/min and at standing time of 5 min at a temperature of 1050°C. The strength

of sintered samples was calculated using 1161°C ASTM standard. a SANTAM device was used in measuring the flexural strength of the sintered samples, and the Micro Vickers method was used to measure the hardness of the samples. Density, porosity, and water absorption was calculated by using Archimedes method.

2.5 Bioactivity

To verify the bioactivity properties of the samples, the SBF simulated body test was used. In this study, as suggested by Kokubo et al. [18], 1 g of each sample was immersed in the solution of a simulated body for 10 days and then rinsed with distilled water several times before drying at 70°C for 12 h. The samples were analyzed under FE-SEM.

3 Results and discussion

3.1 Sample characterization

Figure 1 illustrates the XRD patterns for the as-synthesized HA and CA nanoparticles as well as the nanocomposites synthesized by three different methods. The XRD patterns of as-synthesized HA nanoparticles are shown in Figure 1(1). According to (JCPDS pdf No. 0740-086-00), the diffraction peaks at 2θ of 25.80°, 28.85°, 32.13°, 33.83°, 39.93°, 46.60°, 49.66°, 53.28°, and 63.91° prove the HA nanoparticle formation and demonstrate that other calcium salts have not been formed. After using the XRD data and Scherer equation, the average crystallite size is obtained as 9 nm. The sizes of the as-synthesized HA lattice parameters are obtained as a = 9.424 Å and C = 6.879 Å, indicating that the crystal structure of HA is hexagonal.

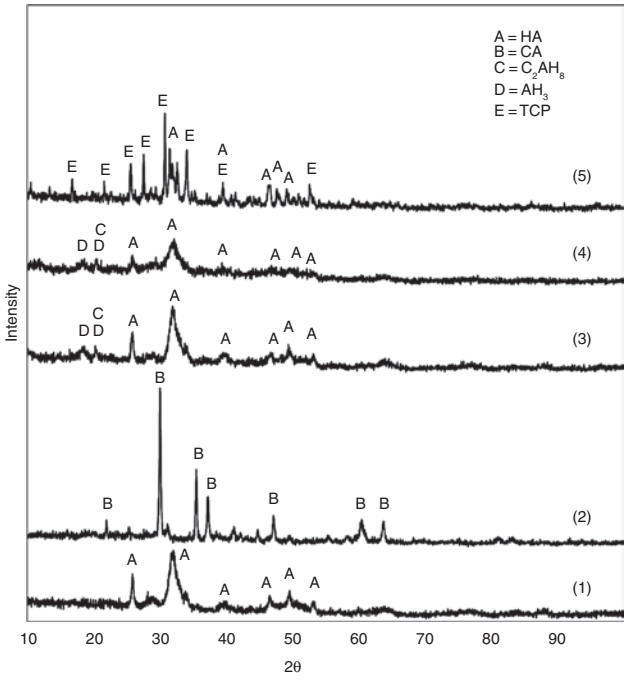

Figure 1: XRD patterns for HA (1), CA, (2) and nanocomposites synthesized by method 1 (3), method 2 (4), and method 3 (5).

Figure 1(2) displays the XRD pattern of the CA nanoparticles. Diffraction peaks at 2θ positions of 21.98°, 30.07°, 35.53°, 37.29°, 47.20°, 60.49°, and 63.72° are assigned to the CA phase in accordance with (JCPDS PDF No. 0134-070-00). Average crystallite size for CA is calculated to be 15 nm. Meanwhile, based on the XRD pattern of the nanocomposite synthesized by method 1 [Figure 1(3)], the diffraction peaks of the HA phase in the 2θ positions of 25.90°, 28.16°, 29.07°, 32.02°, 34.17°, 39.83°, 46.97°, 49.58°, 53.43°, and 64.08° are clearly defined according to (JCPDS PDF No. 0740-086-00). In the XRD pattern of the nanocomposite, reflections related to CA are not recognizable due to the overlapping that occurs with the HA diffraction peaks. The remarkable thing about CA nanoparticles is that they are treated with hydration when they mix with water depending on such conditions as time and temperature durability in water. One of the CA hydration products with a metastable structure is C_2AH_8. This product is usually created at 20°C to 30°C [19]. This phase and the AH_3 phase are observed in the XRD patterns in accordance with (JCPDS PDF No. 0008-012-00) and (JCPDS PDF No. 0146-003-00), respectively. Using Scherer equation, the average crystallite size calculated by the most intense peak is 7 nm.

The XRD pattern of the nanocomposite obtained through method 2 [Figure 1(4)] exhibits similar phases with the samples prepared by method 1. The remarkable thing about this method is that many peaks overlap with one another. Using Scherer equation, the average crystallite size is calculated to be 6 nm. Meanwhile, in the XRD patterns of the synthesized nanocomposites by using method 3 [Figure 1(5)], new diffraction peaks at 2θ of 13.40°, 16.84°, 21.70°, 25.69°, 27.67°, 30.89°, 32.29°, 34.22°, 35.43°, 37. 23°, 39.65°, and 40.85° are observed, thus confirming the presence of tricalcium phosphate as the main phase matched with (JCPDS PDF No. 0941-001-00). This finding may be due to the calcination of the mixture at a high temperature (900°C for 3 h), which causes the conversion of a huge amount of HA to the tricalcium phosphate phase. In the XRD patterns, reflections related to CA were covered by tricalcium phosphate and HA peaks; although it is difficult to detect this phase, EDX data can confirm its presence in the nanocomposite. The average crystallite size determined from the most intense diffraction peak is 32 nm.

The FE-SEM images for the as-synthesized HA and CA nanoparticles and the nanocomposites synthesized

by the three different liquid phase methods are presented in Figure 2. As shown in Figure 2(1), the as-synthesized HA has a narrow particle size distribution in the range of 30 nm–40 nm. In addition, porosity is low and the morphology of particles is spherical. EDX results of as-synthesized HA (Figure 3A) are very close to the calculated values, suggesting that HA is synthesized with high purity. In the HA formula, $Ca_5(PO_4)_3(OH)$, the molar ratio of calcium to phosphate is 1.67, and the molar ratio obtained from EDX data is calculated as 1.60.

The FE-SEM image of the CA nanoparticles [Figure 2(2)] represent spherical particles with narrow size distribution between 35 nm–45 nm. The EDX spectrum of the sample is exhibited in Figure 3B. The Ca/Al molar ratio from the EDX analysis of as-synthesized CA (0.57) is in good agreement with this ratio in the CA formula, $CaAl_2O_4$ (0.5). Meanwhile, the FE-SEM image of the nanocomposite synthesized by method 1 (Figures 2 and 3) displays low porosity, good particle size distribution in the range of 35 nm–40 nm, and spherical morphology. The EDX analysis of the sample (Figure 3C) represents elements that form CA and HA.

According to the FE-SEM image of the nanocomposite prepared by method 2 [Figure 2(4)], particle size distribution is in the range of 45 nm–50 nm, and the morphology of the particles is spherical. In the EDX spectrum of the nanocomposites (Figure 3D), the existence of Ca, Al, and P elements are well confirmed. The FE-SEM image [Figure 2(5)] and EDX spectrum (Figure 3E) of the nanocomposite synthesized by method 3 can be described as follows. The structure and morphology of this nanocomposite is different from those of the two other nanocomposites. This difference is due to the formation of tricalcium phosphate and high-temperature calcination. The composite particles are agglomerated with size distribution of 80 nm–110 nm. They do not have a specific morphology. In the EDX analysis of the nanocomposites, components are well specified, but the calculation of the ratios is difficult due to other phases.

3.2 Physical and mechanical properties

The physical and mechanical properties of HA and other nanocomposites are listed in Table 1. According to Table 1, with the formation of the HA/CA composite, the physical and mechanical properties of HA are changed. Moreover, the nanocomposites have higher density and lower porosity, compared with HA. Reducing porosity in nanocomposites reduces the amount of water absorption in them. The mechanical properties of the nanocomposites are also higher compared with those reported for CA nanoparticles. Among nanocomposites, the nanocomposite synthesized by method 1 has better mechanical properties. Due to the presence of calcium phosphate in the structure of the nanocomposite obtained by method 3, its applications is different from the nanocomposite synthesized by method 1. For example, method 3 can be used as a drug-delivery system, whereas method 1 can be used for implant covers.

For comparative purposes, the structural and mechanical properties of the synthesized HA/CA bioceramic nancomposites and other samples reported in previous studies are summarized in Table 2. As shown in Table 2, all the HA/CA nanocomposites synthesized by liquid phase methods 1, 2, and 3 have smaller particles and better mechanical properties compared with the HA/CA micro-scale composites reported in previous studies [14, 15].

3.3 Bioactivity behavior

By comparing the FE-SEM images of HA nanoparticles before [Figure 2(1)] and after soaking in SBF solution [Figure 4(1)], we can conclude that apatite has grown on HA. The morphology of HA nanoparticles before the bioactivity test is spherical, but after soaking in the SBF solution, it appears as a sponge that represents the growth of apatite. It should be noted that determining the bioactivity behavior of samples by using FE-SEM images is qualitative, although semi-quantitative EDX analysis is commonly used to confirm such a behavior. As the base material in this sample consists of HA nanoparticles and apatite in the SBF test is created on the sample surface, we cannot use semi-quantitative EDX analysis to calculate the approximate amount of apatite growth; however, we can infer from the FE-SEM images that the apatite has grown well on HA nanoparticles and that the nanoparticles have a very good bioactivity.

Meanwhile, the morphology of CA nanoparticles before soaking in the SBF solution [Figure 2(2)] is spherical; after the bioactivity test [Figure 4(2)], it appears in sheeted form, which indicates the presence of apatite. As specified in EDX analysis (Figure 5B), in the nanoparticles of CA that are under the SBF test, some amount of phosphorus is observed due to growth of apatite on its surface. The FE-SEM images of the nanocomposites synthesized by method 1 [Figure 4(3)] show the presence of apatite with sheeted morphology. Such images indicate the good bioactivity properties of the nanocomposites. SEM images of the nanocomposite synthesized by method 2 [Figure 4(4)] also show the presence of apatite, and the morphology

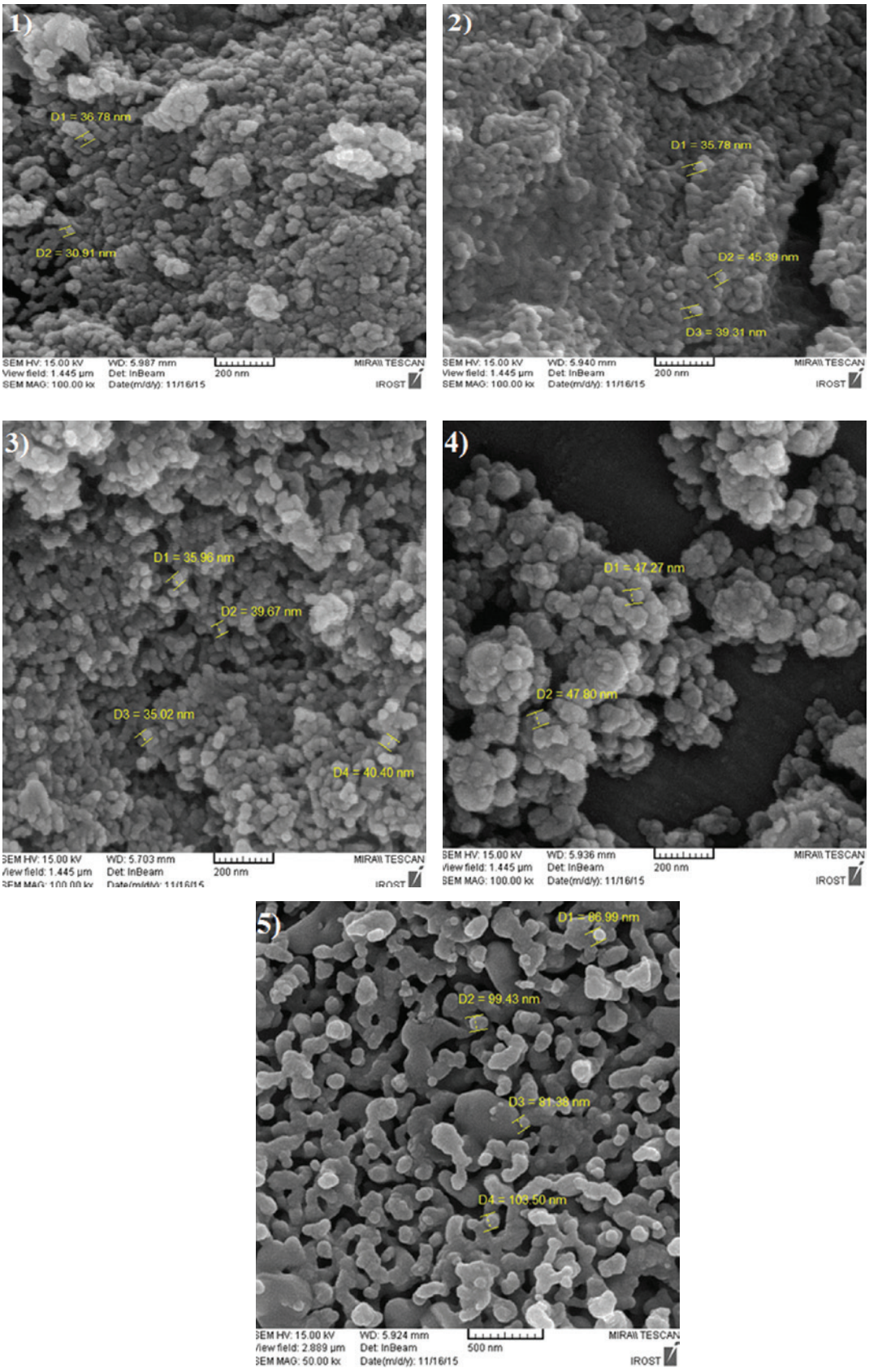

Figure 2: FE-SEM images of samples before immersion in SBF.
(1) HA, (2) CA, (3) nanocomposite obtained by method 1, (4) nanocomposite obtained by method 2, and (5) nanocomposite obtained by method 3.

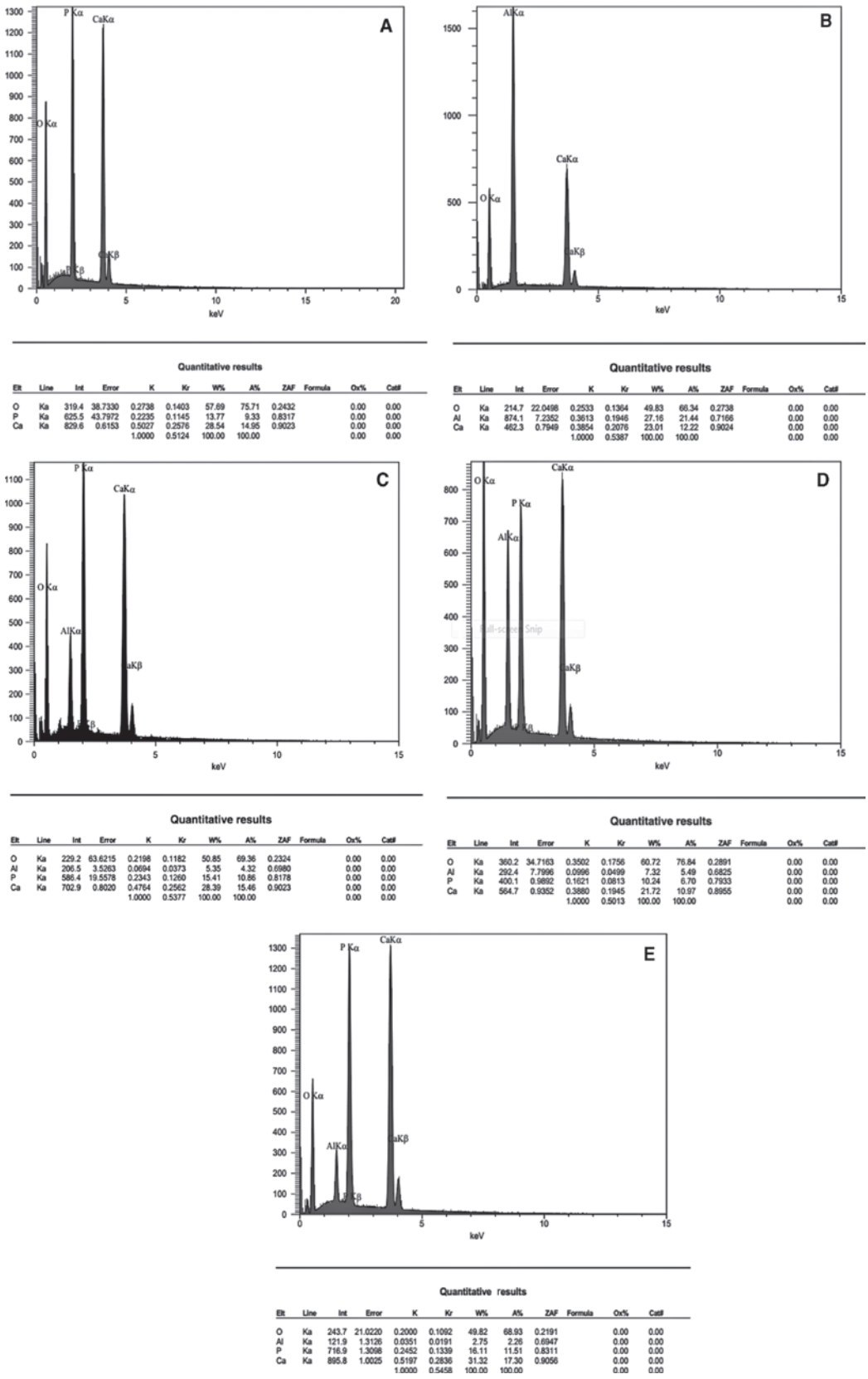

Figure 3: EDX spectra for samples before immersion in SBF.
(A) HA, (B) CA, (C) nanocomposite synthesized by method 1, (D) nanocomposite synthesized by method 2, and (E) nanocomposite synthesized by method 3.

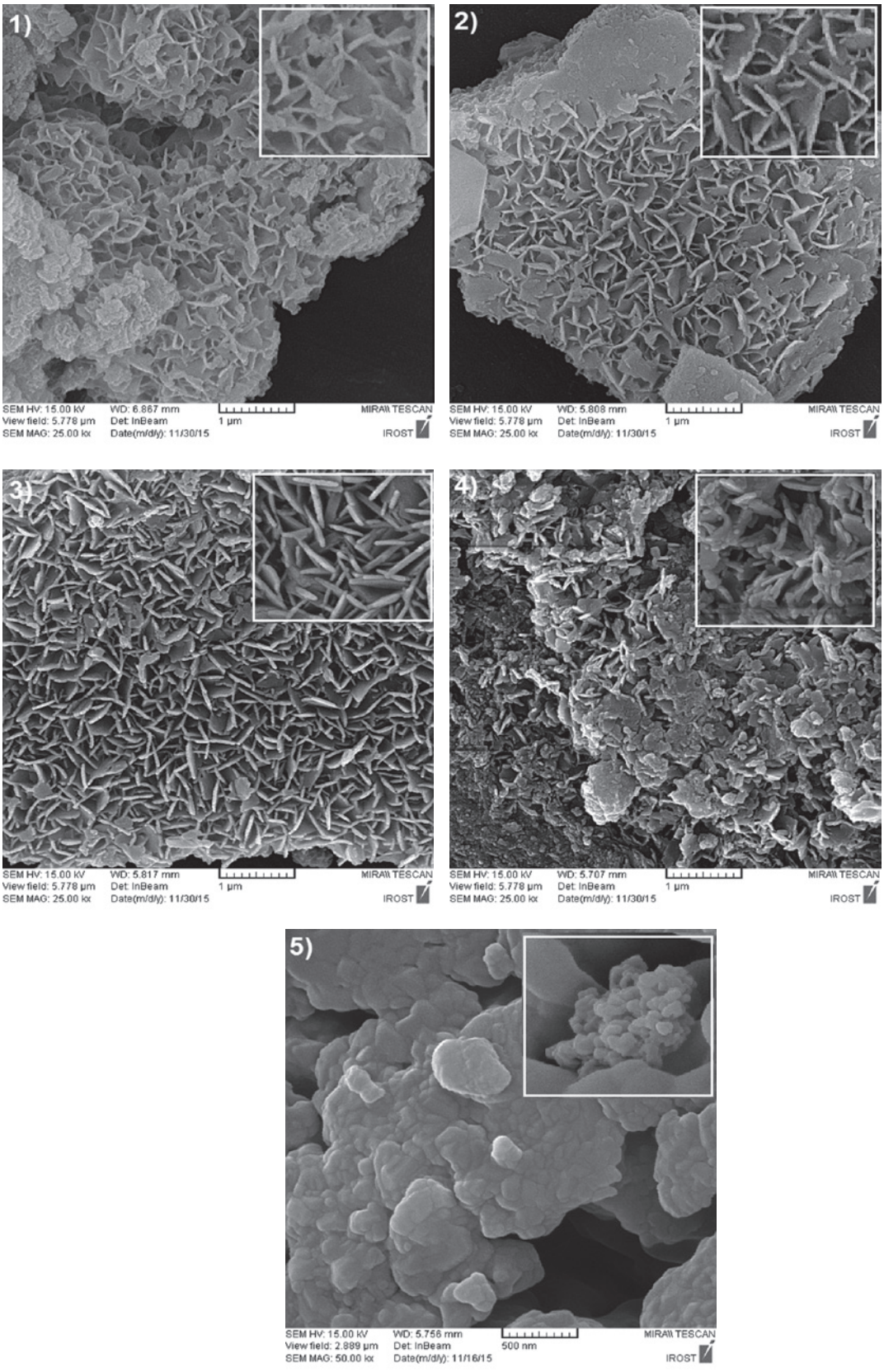

Figure 4: FE-SEM images for samples after immersion in SBF.
(1) HA, (2) CA, (3) nanocomposite obtained by method 1, (4) nanocomposite obtained by method 2, and (5) nanocomposite obtained by method 3.

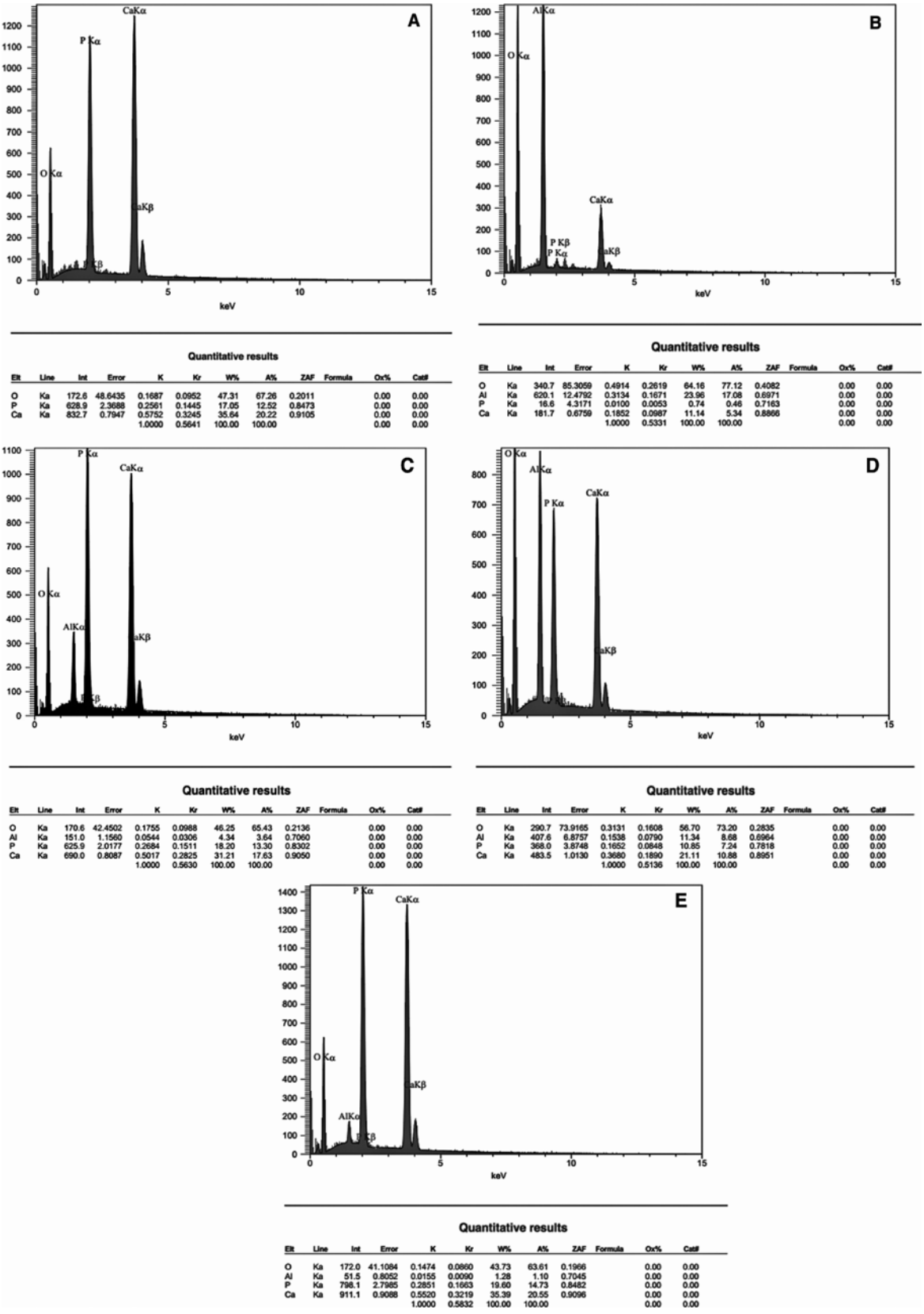

Figure 5: EDX spectra of samples after immersion in SBF.
(A) HA, (B) CA, (C) nanocomposites synthesized by method 1, (D) nanocomposites synthesized by method 2, (E) nanocomposites synthesized by method 3.

Table 1: The physical and mechanical properties of as-synthesized hydroxyapatite and nanocomposites.

Sample	Density	Water adsorption	Porosity	Hardness (H_v)	Flexural strength (MPa)	Compressive strength (MPa)
Hydroxyapatite	3.025	0.29	0.008	124	115	350
Nanocomposite (method 1)	3.11	0.15	0.006	202	135	440
Nanocomposite (method 2)	3.08	0.18	0.007	194	124	400
Nanocomposite (method 3)	3.115	0.14	0.006	200	137	430

Table 2: Comparison of the structural and mechanical properties of the synthesized HA/CA bioceramic nancomposites and samples reported in previous studies.

Sample synthesis method	Average crystallite size	Compressive strength (MPa)	Hardness (H_v)
Method 1	7 nm	440	202
Method 2	6 nm	400	194
Method 3	32 nm	430	200
Mixing HA/20wt.%CA powders (treated at 1250°C) [14]	80 μm (grain size)	330	120
Mechanosynthesis 1–10 wt.%HA/CA cement [15]	~3 μm (average agglomerate size)	>67	–

of the formed apatite is sheeted. Based on the images, apatite formation is sporadic, irregular, and incomplete. The FE-SEM images of the nanocomposites synthesized by method 3 before [Figure 2(5)] and after [Figure 4(5)] the bioactivity tests indicate that the cavities in the images are filled with very small spherical particles. These particles are most likely the apatite formed due to the sample immersion in the SBF solution. Figure 5C–E shows the EDX spectra for the synthesized nanocomposites after immersion in the SBF solution.

4 Conclusion

In comparison with the solid-state method, liquid phase methods used in this work have advantages, such as simplicity, low energy consumption, low-cost, easy control of reaction conditions, easy access to nanoparticles, and environmental compatibility. Moreover, the compressive strength of the synthesized nanocomposites is significantly increased compared with composites reported in previous studies due to the synthesis routes employed [14, 15]. Comparing the SEM images after soaking revealed that the nanocomposites obtained from methods 1 and 3 exhibited good bioactivity. The nanocomposite fabricated via method 1 has a high concentration of apatite. Meanwhile, in the nanocomposite obtained by method 3, as can be seen, all the cavities are filled with apatite and an integrated surface is created. One of the main reasons for the good bioactivity of the nanocomposite synthesized through method 3 is the existence of two phases of HA and tricalcium phosphate in the sample [20]. Apatite growth in the nanocomposite synthesized via method 2 is scattered and incomplete. It should be noted that all results of the FE-SEM images are qualitative; to verify them, semi-quantitative EDX analysis can be used. By using EDX data and FE-SEM images, we can conclude that the nanocomposites synthesized by methods 1 and 3 present good bioactivity, and that the nanocomposite prepared by method 2 has relatively weak bioactivity.

Acknowledgments: The authors wish to thank the Iranian Research Organization for Science and Technology (IROST) for the financial support it has provided.

References

[1] Benaqqa C, Chevalier J, Saädaoui M, Fantozzi G. *J. Biomater.* 2005, 26, 6106–6112.
[2] Li J, Fartash B, Hermansson L. *J. Biomater.* 1995, 16, 417–422.
[3] Zhang C, Zhang X, Liu C, Sun K, Yuan J. *J. Ceram. Int.* 2016, 42, 279–285.
[4] Sopyan I, Fadli A, Mel M. *J. Mech. Behav. Biomed. Mater.* 2012, 8, 86–98.
[5] Radhaa G, Balakumara S, Venkatesanb B, Vellaichamy E. *Mater. Sci. Eng. C* 2015, 50, 143–150.
[6] Ramachandra Rao R, Kannan TS. *Mater. Sci. Eng. C* 2002, 20, 187–193.
[7] Brzezińska-Miecznik J, Haberko K, Sitarz M, Bućko MM, Macherzyńska B, Lach R. *J. Ceram. Int.* 2016, 42, 11126–11135.
[8] Drdlika D, Slamab M, Hadrabac H, Cihlar J. *J. Ceram. Int.* 2015, 41, 11202–11212.

[9] Shojaee P, Afshar A. *J. Surf. Coat. Tech.* 2015, 262, 166–172.
[10] Hannoraa AE, Ataya S. *J. Alloys Compd.* 2016, 658, 222–233.
[11] Shirdara MR, Taherib MM, Moradifarda H, Keyvanfard A, Shafaghatd A, Shokuhfarb T, Izman S. *J. Ceram. Int.* 2016, 42, 6942–6954.
[12] Yugeswarana S, Kobayashib A, Hikmet Ucisikc A, Subramanian B. *Appl. Surf. Sci.* 2015, 347, 48–56.
[13] Mangabhai RJ. Calcium Aluminate Cements, Conf Proceedings. Chapman and Hall (1990).
[14] Beherei HH, El-Bassyouni GT, Mohamed KR. *Ceram. Int.* 2008, 34, 2091–2097.
[15] Oliveira IR, Andrade TL, Araujo KCML, Luz AP, Pandolfelli VC. *Ceram. Int.* 2016, 42, 2542–2549.
[16] Kong LB, Ma J, Boey F. *J. Mater. Sci.* 2002, 37, 1131–1134.
[17] Gaki A, Chrysafi R, Perraki TH, Kakali G. *Chem. Ind. Chem. Eng. Q.* 2006, 12, 137–140.
[18] Kokubo T, Kim HM, Kawashita M, Takadama H, Miyazaki T, Uchida M, Nakamure T. *J. Glastech. Ber. Glass Sci. Technol.* 2001, 73, 247.
[19] Loof J. PhD Thesis, Calcium–Aluminate as Biomaterial: Synthesis, Design and Evaluation. ACTA, Uppsala, University: Sweden (2008).
[20] Lu X, Leng Y. *J. Biomater.* 2005, 26, 1097–1108.

Bionotes

Batool Reyhaniyan Zavareh

Batool Reyhaniyan Zavareh received her Bachelor's degree in Applied Chemistry from the Isfahan University of Technology and her Master's degree in Nanochemistry from the Iranian Research Organization for Science and Technology (IROST). She conducts research on the synthesis and characterization of nanomaterial, such as bioceramic nanostructures.

Alireza Salehirad

Alireza Salehirad is an assistant professor of Inorganic Chemistry at the Iranian Research Organization for Science and Technology (IROST). He has published more than 20 papers in national and international journals. His current research interests include synthesis and characterization of nanomaterials, refractory ceramics, biomaterials and their applications, ceramic and polymer composites, heterogeneous catalysts, inorganic pigments, surface chemistry, adsorbents, and particle technology.

Saeed Mirdamadi

Saeed Mirdamadi is a scientific board member/associate professor at the Iranian Research Organization for Science and Technology (IROST). He received his PhD in Medical Biotechnology from the Institute Pasteur of Iran and continued his career as a researcher at the Pasteur Institute and Medical and Pharmaceutical Group of the Biotechnology Department of IROST. His research focuses on medical biotechnology and microbiology, especially probiotic bacteria and bioactive compounds to identify their effects on health. He has published four patients, and more than 93 scientific papers on the production and formulation of probiotic bacteria, bioactive peptides, and other bioactive compounds. He has also served as supervisor/adviser for more than 100 MSc and PhD theses.